ELSEVIER

Journal of Power Sources 73 (1998) 65–73

JOURNAL OF POWER SOURCES

# Effects of compression on recombinant battery separator mats in valve-regulated lead–acid batteries

K. McGregor *, A.F. Hollenkamp, M. Barber, T.D. Huynh, H. Ozgun, C.G. Phyland, A.J. Urban, D.G. Vella, L.H. Vu

*CSIRO Division of Minerals, P.O. Box 124, Port Melbourne 3207, Australia*

Received 20 August 1997; accepted 26 August 1997

**Abstract**

The spring characteristics of a typical recombinant battery separator mat (RBSM) material used in valve-regulated lead–acid (VRLA) batteries have been monitored at several stages during repetitive deep-discharge cycling service ($C_3$/3, 100% DoD). Through the controlled application of a range of compressive loads, accurate plots of separator thickness vs. compressive force have been recorded for both dry and acid-saturated material. From subsequent analysis, several important properties have been established. Dry RBSM accepts some 'crush' during the first application of pressure. At high levels of force ($\geq$ 60 kPa), RBSM suffers a second stage of crush that can be permanent. Saturation with sulphuric acid solution produces a discernible shrinkage of the material. Thus, for a given thickness of RBSM, an acid-saturated separator will apply less force to the plates than a dry equivalent. This has important consequences for the manufacture of VRLA batteries. In particular, with present separator technology, it would appear that even the use of relatively high levels of compression during the assembly of RBSM VRLA cells is not an effective strategy for attaining the levels of compression required to prevent significant expansion of the positive plates. The difficulties of setting, and then maintaining, adequate levels of plate group compression are further underlined by the promising performance of a constant-compression RBSM VRLA cell. By means of a feedback-controlled system that applies a pressure of close to 40 kPa, this first-of-its-kind cell has displayed relatively stable cycling behaviour. 

*Keywords:* Lead–acid; VRLA; Recombinant battery separator mat; Compression; Resilience

## 1. Introduction

One of the attractive features of valve-regulated lead–acid (VRLA) batteries is that they do not require water addition throughout their lifetimes. This is achieved through the use of Pb–Ca–Sn alloys for the positive grids, together with oxygen-recombination technology. Unfortunately, batteries made from such grids are more susceptible to premature capacity loss (PCL) than traditional cycling batteries, which feature Pb–Sb grids. As a result, the cycle life of VRLA batteries is usually inferior to that of Pb–Sb, flooded-electrolyte equivalents. It is vital that lead–acid technology overcomes this deficiency in order to capture a sizeable share of the rapidly emerging market for electric-vehicle batteries.

In general, the cycle-life of a lead–acid battery that is subjected to repetitive deep-discharge service is limited by the capacity loss suffered by the positive plate. The application of high levels of positive active-material compression within Pb–Sb batteries has been found to improve life cycle significantly [1–7]. For example, highly compressed, flooded-electrolyte batteries with Pb–Sb grids have achieved 3000 cycles to 100% depth-of-discharge (DoD) [5]. Recent studies in the CSIRO laboratories have demonstrated that an appropriate level of compression can offer similar benefits to Pb–Ca-based, flooded-electrolyte systems [8–11]. For instance, the cycle lives of Pb–Ca–Sn cells have been extended significantly through the application of a compressive force of 40 kPa to the plate group. Moreover, the endurance of these cells is found to exceed that of similar Pb–Sb units assembled with conventional, i.e., moderate, levels of compression (8 kPa).

Traditionally, it has been accepted that VRLA cells using recombinant battery separator mat (RBSM) material require a certain level of plate group compression in order to ensure good contact between the RBSM and the battery

* Corresponding author.

0378-7753/98/$19.00 

plates. This provides a sufficient and uniform supply of electrolyte to the plates. Recently, we have recognized that compression also plays an essential role in constraining the expansion of the positive active-material during cycling [8,9]. Such expansion is inherent in plate charge–discharge and, if unchecked, causes a concomitant fall in the packing density of the plate material. This, in turn, lowers the electrical conductivity of the positive mass and leads to a loss of discharge capacity. The severity of the capacity loss depends on the rate and location of the decrease in the apparent density of the active material. (Note, the apparent density is defined as the mass of positive active-material, $PbO_2$, divided by the total volume occupied by the porous structure, i.e., the pore volume is included.) Catastrophic capacity loss is prevented by a certain minimum level of compression, while the maintenance of this compression then determines the long-term performance of the positive plate during charge–discharge cycling.

In RBSM VRLA cells, compression is provided by subjecting the plate group to an external force, prior to insertion into the cell container. This reduces the thickness of the RBSM between the plates and sets up a force that is directed against the plates and cell container. As with any spring material, the magnitude of the force is a function of the displacement of the spring (i.e., the change in thickness of the RBSM) relative to some equilibrium, or reference value. The relationship between the force and the displacement is expressed in terms of a force constant (also known as the spring constant), which is a measure of the stiffness of the spring. For compression in a VRLA battery to be maintained at an appropriate level, the spring constant of the RBSM must be essentially constant throughout the service period. Conversely, changes in spring constant, particularly those that are associated with a reduction of the force for a given displacement, will lead to an overall fall in plate group compression. Unfortunately, such changes are common and are linked closely with loss of cell capacity due to positive-plate expansion. In the absence of published data on how the resilience of RBSM changes during battery service [12], CSIRO and the Advanced Lead–Acid Consortium (ALABC) are conducting a study that is aimed at determining the ability of RBSM to exert and sustain effective compressive forces within VRLA batteries [13]. In this paper, the spring characteristics of typical samples of a commercial RBSM, in both the wet and dry states, are described and analyzed.

## 2. Experimental

In order to investigate the spring properties of RBSM, CSIRO has developed a novel device for the measurement of separator thickness under a range of compressive loads. The apparatus consists of a perspex case in which a piston, driven by gas pressure, is used to apply variable amounts of compression to the RBSM under test. The assembly is referred to as a 'piston-cell'. The piston is attached to a perspex plate that is used to compress a sandwich of eight sheets of RBSM separators and nine PVC spacers. The arrangement of spacers and separators is similar in dimensions to the cell groups used in the charge–discharge cycling part of this study. To control accurately the amount of compression exerted on the separators, the gas pressure that drives the piston is regulated by a pressure control system. By applying a known pressure to the piston, the pressure applied to the separators can be calculated according to a simple formula that relates the piston pressure and area to the separator pressure and area. Schematics of the piston-cell and the pressure control system are shown in Figs. 1 and 2, respectively.

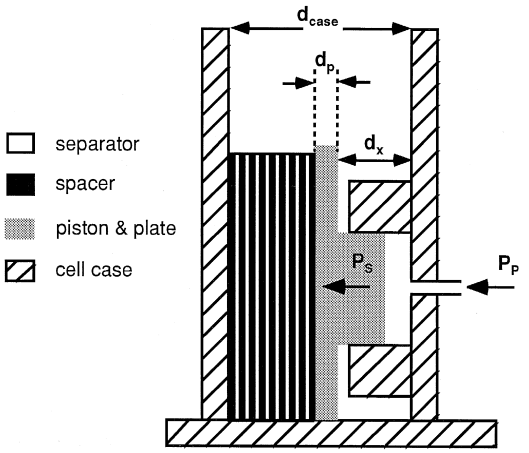


Fig. 1. Piston-cell for the evaluation of RBSM separators under compression.

Compression experiments were conducted by applying pressures of 10–60 kPa, in increments of 5 kPa, to a group of eight dry separators. Measurements of the distance between the piston plate and the inner wall of the cell case were obtained by means of a telescopic gauge and micrometer. The data allowed calculation of the thickness of a separator at a given pressure. The procedure was repeated several times until a reproducible separator thickness was established. The same separators, while subjected to 40 kPa compression, were saturated with $H_2SO_4$ acid (1.286 space gravity) by filling the cell case with acid. After 1 h, the excess acid in the piston-cell was decanted. The compression of acid-saturated separators was then evaluated by the same procedure that was used to test dry separators.

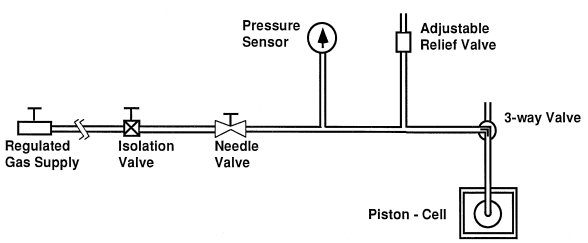


Fig. 2. Pressure control system for compression testing.

Table 1
Constitution of positive and negative pastes

| Constituent | Positive | Negative |
|---|---|---|
| Leady oxide (kg) | 3 | 3 |
| Sulphuric acid, 1.40 space gravity (g) | 280 | 280 |
| Water ($cm^3$) | 390 | 330 |
| Fiber (g) | 0.9 | 1.8 |
| CMC (g) | 7.5 | – |
| Stearic acid (g) | – | 1.8 |
| $BaSO_4$ (g) | – | 11.1 |
| Vanisperse (g) | – | 11.1 |
| Carbon black (g) | – | 6.3 |
| Density (g $cm^{-3}$) | 4.5 | 4.7 |

Separators from cycled cells were removed during dismantling of failed cells and sealed in plastic bags. These separators (or portions of separator) were tested, as outlined above, in the piston-cell.

For selected cells, the plate group was removed at a given stage during service, subjected to analysis of compressive behaviour, and then returned to service. The plate group was placed in a strong plastic bag (to prevent acid drainage) prior to insertion of the group into the piston-cell. Measurements were then taken of compression characteristics by applying pressures of 10 to 40 kPa, in increments of 5 kPa, and recording the corresponding readings of the thickness of the plate group. The procedure was repeated several times until a reproducible plate group thickness was established.

Studies of the effects of compression on a conventional RBSM were conducted in 2 V lead–acid cells. The positive-grid alloys contained 0.076 wt.% Ca, 1.5 wt.% Sn and 0.038 wt.% Ag, while the negative-grid alloys contained 0.075 wt.% Ca and 0.4 wt.% Sn. The grids had the overall dimensions of 126 mm (height) × 150 mm (width) × 1.7 mm (thickness). Pasting was performed by hand, with a PVC paddle; details of the formulation of the positive and negative pastes are given in Table 1. After pasting, each plate was rolled with a 5-kg stainless-steel roller to minimize any local variations in paste loading. The plates were cured at 50°C in 95% r.h. for 24 h, followed by a further 24 h at reduced humidity and the same temperature. The plates were then dried at 75°C in ambient humidity for 24 h. A typical phase composition for the cured state was as follows: 72.5 wt.% $\alpha$-PbO; 27.5 wt.% $3PbO \cdot PbSO_4 \cdot H_2O$ (3BS). The specific surface-area (BET) was 1.38 $m^2\ g^{-1}$.

Cured plates were arranged into 2-V cells that individually were comprised of four positives (each enclosed in two layers of RBSM) and five negatives. The plates were connected to pure-lead terminal posts via spot-welds to pure-lead straps. Each cell group was placed in a container which was constructed from perspex sheet (thickness = 12 mm). All joints were sealed with an acrylic glue and reinforced with stainless-steel screws. The lid was sealed to the top of each container by means of an O-ring. Each cell was fitted with a pressure transducer and a pressure relief valve. The plates were jar-formed, and at this stage, the plates were under virtually no compressive force. At the end of formation, the acid strength was checked and adjusted to 1.285 space gravity

Determination of the phase composition for samples of formed material yielded the following results: 5 wt.% $\alpha$-PbO; 19 wt.% $\alpha$-$PbO_2$; 76 wt.% $\beta$-$PbO_2$. Each of these values is an average of several analyses of samples taken from the upper, middle and lower portions of the plates. The average weights of wet paste for the positive and negative plates were 147 and 140 g, respectively. For positive plates, the mass of $PbO_2$ was determined from the mass of cured material per plate and the phase composition. Based on this information, for each 100 g of cured material, 104.25 g of $PbO_2$ was produced. The mass ratio of negative-to-positive material was 1.2. Therefore, at low-to-moderate rates of discharge, the capacity available from the cells is expected to be determined by the amount of positive material.

After the formation procedure, PVC spacers were inserted into the cells, to provide the required amount of plate compression. The percentage compression of the separator was based on a reference thickness of 1.55 mm (dry) at 10 kPa. For the high-compression cells, an external metal frame was attached to each container to provide the strength needed to withstand the forces associated with relatively high levels of compression.

Charge–discharge performance was characterized by cycling at $C_3/3$. The end-of-discharge voltage was 1.75 V, which corresponds to 100% DoD. The charging procedure involved a constant-current phase (18 A), which was followed by a constant-voltage phase (2.45 V). The latter was maintained until 10% overcharge was returned to the cell. A cell was regarded to have failed once its capacity had fallen to under 50% of the initial value. The discharge capacity for each cell is reported per unit mass of $PbO_2$.

## 3. Characterization of the properties of RBSM

The thickness of a batch of separators was monitored during the application of pressures of between 10 and 60 kPa. A summary of the results is provided in Fig. 3. It is clear that the thickness of the separator in the dry state, obtained during the first compression test (Fig. 3a), was much higher than that recorded during subsequent runs (Fig. 3b). Clearly, the material accepts a degree of ‘crush’ during the first application of compression. Subsequent tests gave consistent thickness–pressure curves (Fig. 3b). During these studies, the maximum level of force (58 kPa) was applied to the dry separators for up to several minutes. At levels of force close to and beyond 60 kPa, some samples suffered a second stage of crush. Importantly, it appears that this compaction can be permanent, i.e., the material does not recover significantly (on the timescale of

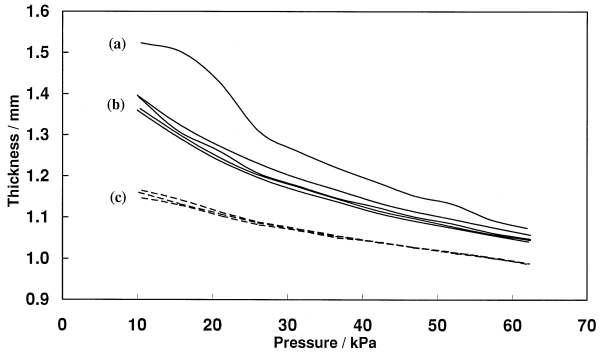


Fig. 3. Thickness of RBSM separators as a function of applied pressure for: (a) dry separators (first run through pressure range); (b) dry separators (second and subsequent runs); (c) separators saturated with aqueous $H_2SO_4$ (1.286 relative density).

hours). Furthermore, tests on a different batch of the same type of separator (not used in cells in this study) showed much less variation in thickness–pressure behaviour between the first and subsequent runs than that observed in Fig. 3. Hence, the performance of RBSM can vary from batch to batch, and may depend on previous treatment (e.g., during manufacturing and subsequent handling).

A distinct shift in the thickness–pressure curve occurred when the sheets of RBSM were saturated with aqueous $H_2SO_4$ (1.286 relative density). The separators were saturated while subjected to a force of 60 kPa. Examination with the piston-cell, over the same range of pressure values, showed that the average thickness of each separator fell significantly, to within the range 1.00 to 1.17 mm, as shown in Fig. 3c. Similar behaviour has been noted previously [14], but no detailed studies have been reported. Fig. 3c demonstrates that, for a given separator thickness, an acid-saturated separator will apply less force to the plates than a dry separator. For example, a thickness of 1.1 mm corresponds to a force of around 50 kPa for a dry separator, but this falls to around 20 kPa for an acid-saturated separator of the same thickness. The drop in pressure is probably caused by adhesion between the electrolyte-soaked glass-fibers due to the effect of surface tension [14] (K. Micka, J. Heyrovsky Institute of Physical Chemistry, Prague, Czech Republic, 1997, private communication). Consequently, the fibers behave as if they are 'glued' together. Importantly, the slope of the curve in Fig. 3c shows that relatively small changes in separator thickness (perhaps due to some distortion of the cell container) could cause a significant decrease in the force applied to the plates.

Before discussing further the role of RBSM in determining plate group compression, it is useful to consider the approach taken by the battery industry in defining the term 'compression'. Unfortunately, there is at present no universal, standard definition of compression. Nevertheless, compression is commonly reported as a percentage reduction in thickness, with respect to some reference thickness; i.e., as a dimensionless parameter, rather than as a force or pressure. On this basis, the Battery Council International (BCI) has issued a standard method for the determination of the thickness of RBSM separator material. According to the BCI standard, the reference value for thickness is that measured under a load of 10 kPa [15]. From this, values of compression (%) are calculated as follows:

$$C_{s_x} = 100\left[\left(d_{s_{10}} - d_{s_x}/d_{s_{10}}\right)\right] \quad (1)$$

where: $C_{s_x}$ = compression (%) of the separator at test pressure; $d_{s_x}$ = thickness of the separator at test pressure; $d_{s_{10}}$ = thickness of the separator at 10 kPa.

Values of separator thickness, wet and dry, and at different levels of compression, are collected in Table 2. The thickness at 10 kPa, as determined by means of the piston-cell, is 1.55 mm; this is based on the separator thickness on the first run through the pressure range. It can be seen from Table 2 that the separator thickness obtained for the same nominal force differs according to the method employed for the measurement of thickness. This problem has also been discussed in a recent paper by Zguris [16]. We suggest that the piston-cell provides the most valid measurement of separator thickness, since the arrangement and dimensions of the separators and PVC spacers are more representative of actual cell conditions.

Table 2
Properties and characteristics of a conventional RBSM separator

| Property | Result | Method |
|---|---|---|
| Density (g $m^{-2}$) | 220 | – |
| *Thickness (mm)* | | |
| *10 kPa* | | |
| Dry | 1.52 | TMI 553[a] |
| Dry | 1.567 | Messmer[a] |
| Dry | 1.551 | Piston-cell |
| Acid-saturated | 1.348 | Piston-cell |
| *20 kPa* | | |
| Dry | 1.282 | Messmer[a] |
| Dry | 1.301 | Piston-cell |
| *40 kPa* | | |
| Dry | 1.199 | Piston-cell |
| Acid-saturated | 1.151 | Piston-cell |
| *Pore size ($\mu$m)* | | |
| Maximum | 30 | Kerosene[a] |
| Minimum | 3.4 | Coulter[a] |
| Maximum | 46.6 | Coulter[a] |
| MFP | 6.1 | Coulter[a] |
| Average | 35.4 | Multipoint BET ($N_2$) |
| *Specific surface-area ($m^2$ $g^{-1}$)* | | |
| | 1.06 | Hollingsworth & Vose, Method No. OP-A-142[a] |
| | 1.35 | Multipoint BET ($N_2$) |

[a] Test performed by Hollingsworth & Vose.

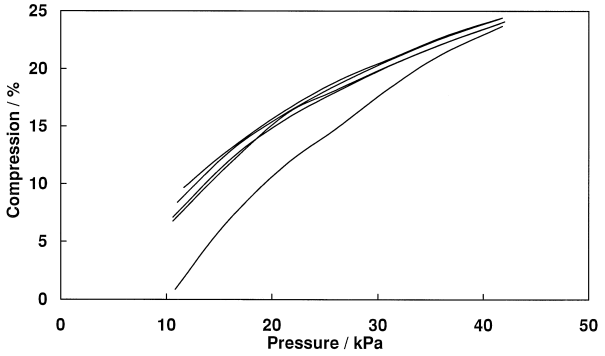


Fig. 4. Compression of dry RBSM separators as a function of applied pressure and based on a reference thickness of 1.55 mm at 10 kPa.

Based on the reference value of 1.55 mm, a plot of compression (%) as a function of applied pressure was constructed for a dry separator (Fig. 4). For this evaluation, the maximum level of compression was limited to around 40 kPa, rather than 60 kPa, as in Fig. 3. In doing this, it was found that less crushing of the separator took place. It is now possible to compare the levels of compression employed in the industry with our data on RBSM behaviour. Fig. 4 shows that for a dry separator, a maximum of 24% compression is achieved at a pressure of 42 kPa. This percentage value of compression can be compared with the values used in the assembly of VRLA cells; the compressive loads used in commercial practice are around 25–30%. Importantly, once a cell assembled with 42 kPa is filled with electrolyte, the pressure within the plate group will fall. The data in Fig. 3, which can be used as a guide here, suggest that compression will fall to around 10 kPa. As noted earlier, values of this order are usually not sufficient to ensure even moderate life-cycle.

## 4. Charge–discharge cycling studies

Repetitive charge–discharge cycling ($C_3/3$, 100% DoD) of a series of low- and high-compression cells was conducted. The low-compression cells (LCl) were assembled with a nominal 15 kPa (5%) compression, while the high-compression cells (HCl) were subjected to an initial plate group compression of ~50 kPa (30%). These values are for separators in the dry state.

The specific capacity performance for representative low- and high-compression cells is shown in Fig. 5. In the early stages of cycling, the positive active-material utilization for cell LCl was in the region of 35 to 40%, but the discharge capacity began to fall steadily from the third cycle. Between cycles 3 and 20, the capacity fell by ~20%. Cell service was terminated at cycle 78, after the capacity had fallen below 50% of the initial value. Regular monitoring of the potential of the positive plate showed that the loss of capacity was due solely to a decline in the performance of the positive plates.

Given the relatively low level of plate compression that was set for cell LCl, the degradation in capacity is consistent with unrestrained expansion of positive material that resulted in loss of conductivity and, ultimately, isolation of significant portions of plate material. X-ray diffraction (XRD) phase analysis results revealed a relatively simple phase composition, i.e., samples taken from nine locations throughout the plate consisted mostly of $\beta$-$PbO_2$. This analysis of the failure mode is supported by findings from scanning electron microscopy (SEM) investigations, as well as by the observation of large-scale shedding of the positive material during the disassembly of the cell, particularly from the lower parts of the plates. By contrast, the negative plates appeared to be in a relatively healthy condition. It is likely that stratification made only a small contribution towards capacity loss. Measurements of electrolyte relative density revealed a difference of 75 points between samples taken from the top and the bottom of the cell (as expected, smaller differences were found in the upper regions of the cell). In addition, this cell contained considerable excess of electrolyte, as a result of the low compression and the large inter-plate spacing.

A plot of the specific capacity vs. the cycle number for cell HCl is also given in Fig. 5. The specific capacity for cell HCl rose steadily in the early stages of cycling, and reached a peak value at cycle 20. From that point, there was a gradual decrease in capacity. At cycle 60, a malfunction occurred in the charging control equipment. After repairs and complete recharging of the cell (over a period of 24 h), the capacity of the cell returned to its previous levels. Within five cycles, however, the capacity began to fall again at a severe rate. From cycle 84 to 89, cell HCl was inverted, in order to test for the possible development of electrolyte stratification. A small increase in capacity was observed. At the completion of cycle 89, by which point the capacity had fallen by around 25% of its peak value (cycle 20), the entire plate group was removed from the cell for several hours and subjected to compression

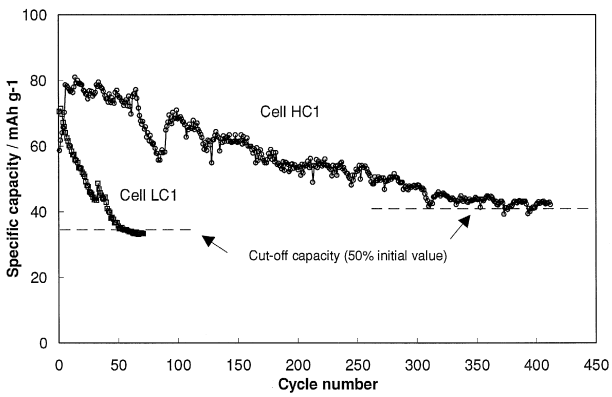


Fig. 5. Specific discharge capacity vs. cycle number for cells LCl and HCl.

testing by means of the piston-cell (these results are discussed in Section 6).

After compression testing, the plate group of cell HCl was returned to its container, reconnected to the charge–discharge control system, and then charged for a short period. On recommencing cycling, a significant increase in cell capacity was observed, namely, from 58 mA h $g^{-1}$ at cycle 89 (before compression testing) to $\sim$70 mA h $g^{-1}$ (cycle 95 to 100); at the latter level, the capacity was close to 90% of the peak value recorded early in service. Such increases in capacity are a common feature for all cells subjected to in situ compression testing; the reasons for this behaviour are unclear and require more investigation. Subsequently, the cell capacity decreased at the same rate observed prior to the malfunction, and service was eventually terminated at cycle 412 (50% capacity loss). The total weight loss from the cell was $\sim$7 g.

On the basis of XRD phase analysis, SEM and other post-service analyses similar to those described for cell LCl, the failure of cell HCl is also attributed to the gradual expansion and redistribution of the positive material during cycling. Support for this explanation was also provided by measurements of positive-plate thickness for cell HCl from low-magnification SEM images. These revealed an appreciable increase in thickness, from close to 2.2 mm (prior to service) to between 2.5 and 2.8 mm (end of service). The thickness of each negative plate increased slightly ($<0.1$ mm) as well. Measurements of electrolyte specific gravity for cell HCl revealed only a small difference between the values for upper and lower regions of the separator (0.034 space gravity). Thus, it appears that stratification made only a minor contribution to capacity loss.

## 5. Compression studies

The plate group of cell HCl was removed at selected stages during service, subjected to an analysis of compressive behaviour in the piston-cell, and then returned to service. Plots of plate group thickness vs. applied force are presented in Fig. 6 for: (a) a freshly formed plate group of the design used for the HC-series cells; (b) cell HCl at cycle 89 (25% capacity loss); (c) cell HCl at cycle 412 (50% capacity loss). For clarity, only the second and subsequent runs are reported in Fig. 6. The difference between the data for the first and second/subsequent applications of pressure was similar to that observed for fresh RBSM (see Fig. 3).

Inspection of the plots in Fig. 6 reveals that the behaviour of the plate group in cell HCl differs from that of a freshly formed equivalent. Over the same range of applied pressure, the changes in plate group thickness for cell HCl (Fig. 6b,c) are relatively small compared with those for the formed cell (Fig. 6a), as shown by the differing slopes of the plots. The change in thickness is particularly evident for the cell HCl plate group at the end of service life (Fig. 6c), and indicates that there has been an increase in the spring constant of the separator, i.e., the displacement of the spring (separator) under the same force is now smaller than that observed originally. It is also important to compare the thickness of the two plate groups at the standard reference value (10 kPa). The thickness of the plate group decreases during the early stages of cycling (Fig. 6a,b). This is probably due to compaction of the RBSM, in a fashion similar to that described earlier for dry separators. Between cycle 89 (Fig. 6b) and cycle 412 (Fig. 6c), the plate group increased in thickness, presumably due to the expansion of the positive plates and concomitant crushing of the separator. Post-service examination of the positive plates, reported earlier, support this explanation. Given that the plate group thicknesses (formed and cycled) are all within 1 mm, the increase in plate thickness for the cycled cell has been 'matched' to a large degree by a decrease in separator thickness.

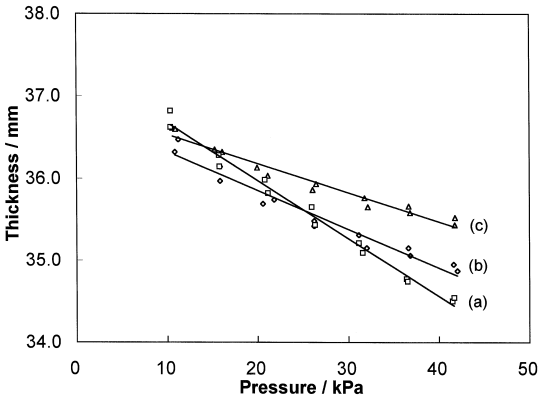


Fig. 6. Thickness of: (a) freshly formed plate group; (b) cell HCl plate group, cycle 89, 25% capacity loss; (c) cell HCl plate group, cycle 412, 50% capacity loss.

These changes in compression properties have important implications for cell characteristics. Perhaps most importantly, cycle-to-cycle variations in the thickness of plates, due to the well-known expansion and contraction of plate material, would have caused the amount of compression within HCl to vary considerably during service; certainly more than at the start of service. For this cell, the reduction in thickness of the RBSM at a given applied force demonstrates that the material has relaxed to a certain extent during service life, and has allowed the progressive expansion of the porous mass. This is a well-known characteristic of many spring materials when they are held under compression for prolonged periods. The dynamic properties of the material are altered and, as a consequence, the positive material is provided with less constraint.

Fig. 7 shows piston-cell data (thickness vs. applied pressure) for separators from the low-compression cell LCl at the completion of service (78 cycles, 50% capacity loss). Following the initial pass through the range of pressures (Fig. 7a), replicate measurements (Fig. 7b)

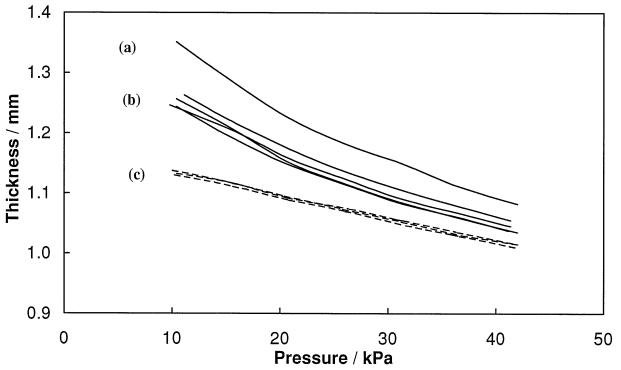


Fig. 7. Thickness of separators from cell LCl after failure, as a function of applied pressure: (a) separators as removed from cell (first run); (b) separators as removed from cell (second and subsequent runs); (c) separators re-saturated with aqueous $H_2SO_4$ (1.286 relative density).

yielded reproducible data for separator thickness. In the second phase of the investigation, the separators were resaturated with aqueous $H_2SO_4$. This step was taken because it was suspected that a significant proportion of the electrolyte originally present had drained out during removal from the cell. Fig. 7c shows that, upon re-saturation, a distinct contraction occurred. The thickness at 10 kPa, for example, fell from 1.25 to 1.15 mm. Further, the complete thickness–pressure curve is virtually the same as that observed for fresh (unused) separators under the same conditions (Fig. 7c). [This was verified by plotting curves for fresh material and cycled material (see Fig. 8) on the same axes.] Therefore, it appears that no real degradative changes occurred in this particular batch of separators during 78 cycles at $C_3/3$, under relatively low compression.

The same tests were also performed on separators from the high-compression cell HCl, and Fig. 8 provides a summary of the characteristics of the separators at the completion of 412 $C_3/3$ cycles. For clarity, only the second and subsequent runs are reported in Fig. 8. It is noted that the average thickness (Fig. 8c) is appreciably less than that of the separators from cell LCl (Fig. 8b). Clearly, the combination of the increase in the thickness of the positive plates with cycling, noted above, and the higher level of compression employed for cell HCl has led to a significant reduction in separator thickness. Interestingly, the slopes of the lines drawn through each of the thickness–pressure plots in Fig. 8 are almost identical. This suggests that the spring constants of both the low- and high-compression RBSM samples are very similar to that of fresh saturated material. By contrast, in situ compression studies (Fig. 6) for cell HCl demonstrated that changes in the separator spring constant were evident during service. One explanation may be that since a number of weeks elapsed between cell tear-down and post-service compression testing, the separators experienced some recovery in their spring properties. Further studies, aimed at shedding more light on this matter, are in progress.

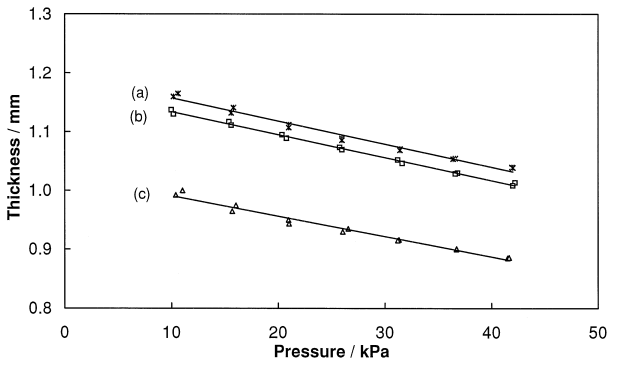


Fig. 8. Thickness of separators, removed from cells and re-saturated with aqueous $H_2SO_4$, as a function of applied pressure: (a) fresh saturated; (b) cell LCl, 78 cycles, 50% capacity loss; (c) cell HCl, 412 cycles, 50% capacity loss.

A second noteworthy feature concerns the results of the re-saturation of the separators of cell HCl. Comparison of the data shows that there was little difference in the thickness–pressure curves for the separators of cell HCl before and after re-saturation with aqueous $H_2SO_4$. By contrast, as noted earlier, re-saturation of the separators from cell LCl resulted in a marked contraction (Fig. 7c). These results illustrate another effect of a higher level of compression on separator properties.

## 6. Advanced compression management

For cells operated with a fixed-plate interspacing, the amount of separator compression is not actively controlled during charge–discharge cycling and, based on the findings presented earlier in this paper, can be expected to vary significantly from cycle-to-cycle. Moreover, any relaxation of the separator can result in a decrease in both separator compression and the force applied to the plate group. To allow accurate control over plate group compression, a second generation piston-cell, 'piston-cell II', has been designed and built (A.F. Hollenkamp et al., manuscript in preparation). In this apparatus, a piston, driven by gas pressure, is used to apply constant amounts of compression to the cell group. A feedback-control circuit maintains the compression at a pre-set level. In-house software has been written to control the compression level, and to measure and record the cell voltage, current, charge–discharge capacity, and plate group thickness.

Repetitive $C_3/3$ (100% DoD) cycling of the first constant-compression VRLA cell, CCl, is in progress. The separator employed in cell CCl, supplied by Hollingsworth & Vose as a part of a wider collaborative study, is similar to that used in cells LCl and HCl, but has a higher specific surface area (2.2 vs. 1.06 $m^2\ g^{-1}$). A plot of the specific capacity vs. cycle number for cell CCl is shown in Fig. 9. For this cell, the compression has been fixed at a constant level of $40 \pm 0.2$ kPa during charge–discharge cycling.

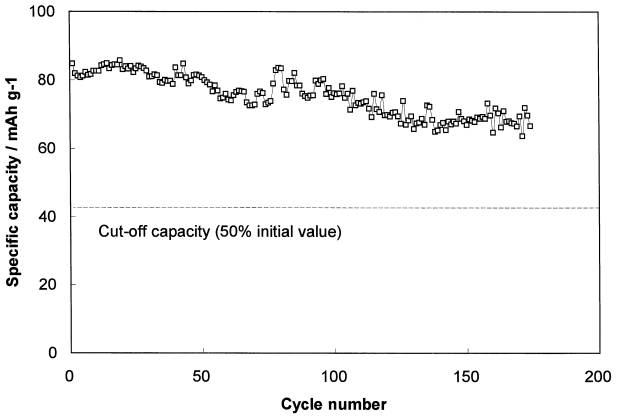


Fig. 9. Specific discharge capacity vs. cycle number for constant-compression cell, CCl.

The plot illustrates that the capacity of cell CCl remained reasonably steady over the first 100 cycles, and gradually declined to around 80% of its nominal capacity by cycle 140. Cell CCl has maintained this level of capacity steadily since that point, and has completed 170 $C_3/3$ cycles.

The performance of the constant-compression cell CCl is in marked contrast to that displayed by the other high-compression VRLA cells, where, in general, the capacity increased and reached a peak at around cycles 10 to 20 (for a typical plot see Fig. 3), before declining steadily. Moreover, cell HCl suffered substantially more capacity loss at similar stages of cycle life. In the earlier cells, which were operated with a fixed inter-plate spacing, the amount of separator compression was not actively controlled during charge–discharge cycling, and was no doubt substantially less than 40 kPa. The results obtained here with cell CCl suggest that overcoming variations in compression during service life, via the application of a constant and uniform force on the active material, is a vital factor if VRLA cells are to maintain good capacity under deep-discharge cycling.

## 7. Conclusions

An analysis of the compressive behaviour of a batch of conventional RBSM material has revealed that its spring characteristics can be altered by: (1) the addition of acid (i.e., wetting) which causes contraction of the separator; (2) relatively high compressive loads, which can induce permanent crushing of the material. For a given separator thickness, an acid-saturated separator applies less force to the plates than a dry separator. Furthermore, small variations in compression and separator thickness can have a large impact on the amount of force that is actually applied to the plates. These results indicate that great care must be taken in the assembly of VRLA cells that employ RBSM separators.

In situ compression testing of the plate groups of cells assembled with high initial levels of compression reveals that the separators are crushed considerably by the progressive expansion of the positive material. Furthermore, cycle-to-cycle variations in the thickness of the plates can cause the amount of compression to vary considerably during service. These studies suggest that conventional VRLA separators, deployed in cells with fixed inter-plate spacing, cannot maintain the levels of compression required to prevent significant expansion and redistribution of the active material during repetitive $C_3/3$ cycling. The finding that RBSM, once removed from long-term cycling, recovers its original resilience to a large degree, is interesting but of no practical consequence.

A VRLA cell subjected to a constant compression of 40 kPa has suffered substantially less capacity loss, at similar stages in service life, than cells with fixed inter-plate spacing. It appears that removing the variations in compression associated with fixed plate spacing, via the application of a constant and uniform force on the active material, is an important factor if VRLA cells are to sustain a good level of discharge capacity under deep-discharge cycling.

## Acknowledgements

The support of the Advanced Lead–Acid Battery Consortium, through funding for Project AMC-009, is gratefully acknowledged. The authors wish to thank their colleague D.A.J. Rand for his critical reading of the manuscript and for stimulating discussions.

## References

[1] K. Takahashi, M. Tsubota, K. Yonezu, K. Ando, J. Electrochem. Soc. 130 (1983) 2144.
[2] J. Landfors, J. Power Sour. 52 (1994) 99.
[3] S. Atlung, B. Zachau-Christiansen, Degradation of the positive plate of the lead/acid battery during cycling, J. Power Sour. 30 (1990) 131.
[4] J. Alzieu, B. Geoffrion, N. Lecaude, J. Robert, Proc. Fifth Int. Vehicle Symp., EVS-5, Com. 783205, Philadelphia, October 2–5, 1978, Electric Vehicle Council, 90 Park Avenue, New York, NY, USA.
[5] J. Alzieu, J. Robert, Cycle life of stressed lead–acid batteries, J. Power Sour. 13 (1984) 93.
[6] J. Alzieu, N. Koechlin, J. Robert, J. Electrochem. Soc. 134 (1987) 1881.
[7] D. Pavlov, Effect of dopants (Group Va) on the performance of the positive lead/acid battery plate, J. Power Sour. 33 (1991) 221.
[8] A.F. Hollenkamp, When is capacity loss in lead/acid batteries 'premature'?, J. Power Sour. 59 (1996) 87.
[9] A.F. Hollenkamp, R.H. Newnham, Benefits of controlling plate group expansion: opening the door to advanced lead–acid batteries, J. Power Sour. 67 (1997) 27.
[10] A.F. Hollenkamp, K.K. Constanti, M.J. Koop, K. McGregor, AL-

ABC Project AMC-003, Final Report, April 1993–March 1995, CSIRO Div. Minerals, Melb., Commun. DMR-031, May 1995.
[11] R.H. Newnham, W.A.G. Baldsing, R.D. Bramley, J.A. Hamilton, C.G. Phyland, D.G. Vella, L.H. Vu, ALABC Project AMC-007, Progress Report 4, August–October 1996 (Annual Report), CSIRO Div. Minerals, Melb., Commun. DMR-412, November 1996.
[12] K. Peters, Review of factors that affect the deep cycling performance of valve-regulated lead/acid batteries, J. Power Sour. 59 (1996) 9.
[13] ALABC Project AMC-009, December 1995–November 1997, Int. Lead–Zinc Res. Organization, Research Triangle Park, NC, USA.
[14] K. Nakamura, M. Shiomi, K. Takahashi, M. Tsubota, Failure modes of valve-regulated lead/acid batteries, J. Power Sour. 59 (1996) 153.
[15] Battery Council Int. Standard Test Method for Thickness of Recombinant Battery Separator Mat, Section II34, pp. 1–4.
[16] G. Zguris, A review of physical properties of separators for valve-regulated lead/acid batteries, J. Power Sour. 59 (1996) 131.